

## Pathogenesis of Limb Malformations in Mice Induced by Methoxyacetic Acid

Chairuddin RASJAD, Keisuke YAMASHITA, Abdul Razak DATU and Mineo YASUDA

*Department of Anatomy, Hiroshima University School of Medicine, Kasumi 1-2-3, Minami-ku, Hiroshima 734, Japan*

### ABSTRACT

The present study was performed to reveal the pathogenesis of limb malformations induced by methoxyacetic acid (MAA) in developing mouse limbs. Pregnant Jcl:ICR mice were orally given at gestational day (gd) 10.5, 11.0, or 11.5 (vaginal plug = gd 0) a single dose of MAA 10 mmol/kg of body weight. Various patterns of cell death in limb buds were observed by vital dye staining with Nile blue A. Under a light microscope and transmission electron microscope, excessive cell death was observed in the mesenchyme as well as in the apical ectodermal ridge (AER) 2 hr after MAA treatment, reaching a maximum after 6 hr. Scanning electron microscopic examinations showed hypoplasia of the AER and small hand plates 24 hr after treatment. Small hand plates and delayed digital ray formation were noted at 48 hr. Neither detachment nor massive necrosis was detected in the periderm covering the limb bud. The distribution of cell death 6 hr after treatment was similar in limb buds treated either at gd 10.5, 11.0 or 11.5, but the final pattern of limb defects was different in fetuses treated at different stages. This study indicates that variations in the pattern of limb defects induced by MAA are due to differences in the amount and distribution of cell death, together with differences in the regenerative capacity of surviving cells.

**Key words:** *Plasticizers, Cytotoxic effects, Cell death*

Methoxyacetic acid (MAA), one of the metabolites of di(2-methoxyethyl) phthalate (DMEP)<sup>1)</sup>, is a potent teratogen in mice. We found that MAA given at different developmental stages induced various patterns of limb defect<sup>3)</sup>.

Recently, a staging system for developing mouse limbs<sup>6)</sup> was devised, and fate maps of mouse limb buds were constructed using exo utero surgical techniques and carbon particle injections<sup>2)</sup>. The staging system and fate maps enable us to correlate initial pathological changes in early limb buds treated with a teratogen through to final defects.

The present study aims at revealing the initial pathological changes induced by MAA, correlated to the final limb defects which were described in detail in our previous paper<sup>3)</sup>.

### MATERIALS AND METHODS

Colony bred Jcl:ICR mice from CLEA Japan, Inc. were used in the present investigation. Mature females were placed with males overnight. Copulation was ascertained by the presence of a vaginal plug on the following morning, and 0.00 A.M. of that day was denoted as the start of day 0 of gestation (gd 0).

Pregnant mice were given a single oral dose of MAA (supplied by Katayama Chemical, Japan) at 10 mmol/kg of body weight dissolved in distilled water at gd 10.5, 11.0, or 11.5. Controls for these experiments were treated with comparable volumes of distilled water at the corresponding time points. Examinations were made at intervals ranging from 2 to 72 hr after treatment using Nile blue A supravital staining, light microscopy, scanning electron microscopy and transmission electron microscopy. Embryonic limbs were staged according to Wanek et al<sup>6)</sup>.

#### Nile blue A supravital staining

Nile blue A sulfate, a lysosomotropic vital dye, was used to identify areas of cell death in treated and control embryos. The embryos with their membranes removed were placed in a 1:20,000 Nile blue A (supplied by Allied Chemical Ltd.) in Hanks' solution at 37°C for 30 min to 1 hr and photographed utilizing a dissecting microscope with a camera.

#### Light microscopy

Embryos were fixed in Bouin's solution. Limb buds were dissected out, embedded in paraffin and sectioned parallel or perpendicular to the palmar plane at 7  $\mu$ m thickness. The sections were stained

with haematoxylin and eosin, and were observed under a light microscope.

#### Scanning electron microscopy

Embryos were fixed in 2.5% glutaraldehyde in Hanks' solution, adjusted at pH 7.2. Limbs were excised and dehydrated through a graded series of ethanol and infiltrated with isoamyl acetate. The specimens were dried from liquid CO<sub>2</sub> in a Hitachi HCP-1 critical point dryer, mounted on aluminium stubs, coated with gold in an EIKO IB-3 sputter coater, and observed utilizing a Hitachi 430 scanning electron microscope.

#### Transmission electron microscopy

Limbs were fixed in 2.5% glutaraldehyde as above and postfixed with 1% OsO<sub>4</sub> in Hanks' solution at pH 7.2, dehydrated through a graded series of ethanol, placed in propylene oxide, and embedded in EPOK 812 (Oken Shoji, Japan). Thin sections were cut with a Sorvall MT-1 ultramicrotome, stained with uranyl acetate and lead citrate, and observed in a JEOL 1200 EX-type transmission electron microscope. Sections about 1  $\mu$ m thickness were also cut, stained with toluidine blue, and examined by light microscopy.

## RESULTS

### Nile blue A supravital staining

Figure 1 displays the configuration of Nile blue A in the forelimb buds at gd 10.5. In the control series, dye uptake was observed only in the zones of physiological cell death (Fig. 1 B). In MAA treated series, no abnormal uptake of dye was detected 2 hr after treatment. At 4 hr excessive uptake of dye was observed (Fig. 1 E) and the maximal uptake of Nile blue A was found 6 hr after treatment at gd 10.5, 11.0, or 11.5 (Fig. 1 C, D, F, G, H, for gd 10.5). The distribution of dye was observed diffusely in the distal half of the hand plate, and the preaxial area showed stronger uptake than the postaxial area. The same tendencies were observed generally among the groups treated at different developmental stages, although there were some differences in the uptake at the zones of physiological cell death among specimens at different stages, and subtle differences in distribution of dye even among specimens treated at the same developmental stages (Fig. 1 C, D, G, H). When the dye distribution was compared between the fore- and hindlimbs, no specific differences were noted.

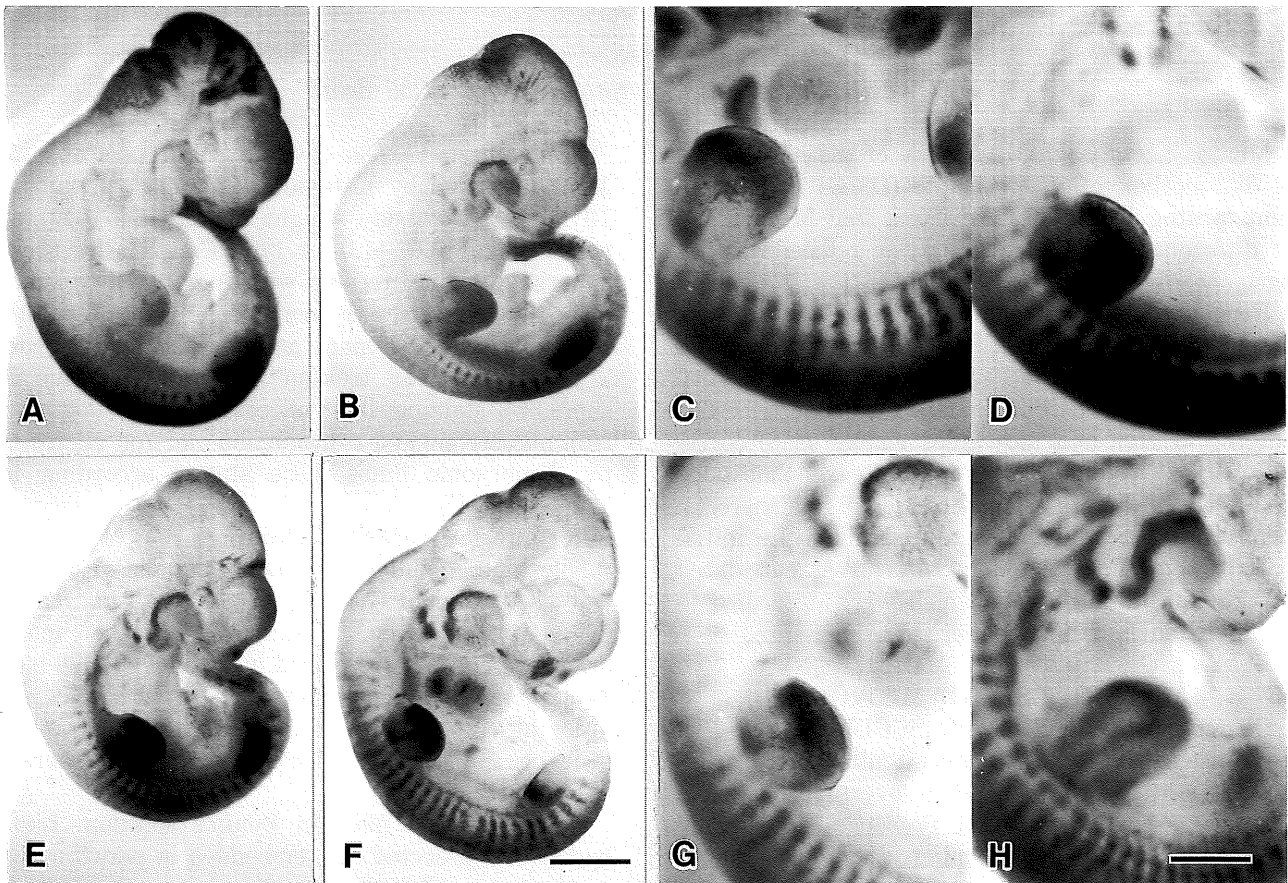


**Fig. 1.** Nile blue A supravital staining of forelimb buds treated at gd 10.5, 4 hr and 6 hr after treatment.

A, B: Control series; C - H: Treated series.

A, E: 4 hr; B, F 6 hr; C, D, G, H: 6 hr after treatment.

Note variations in distribution of dye uptake on the limb bud.

Scale bars = 1 mm for A, B, E, F, and 0.5 mm for C, D, G, H, respectively.

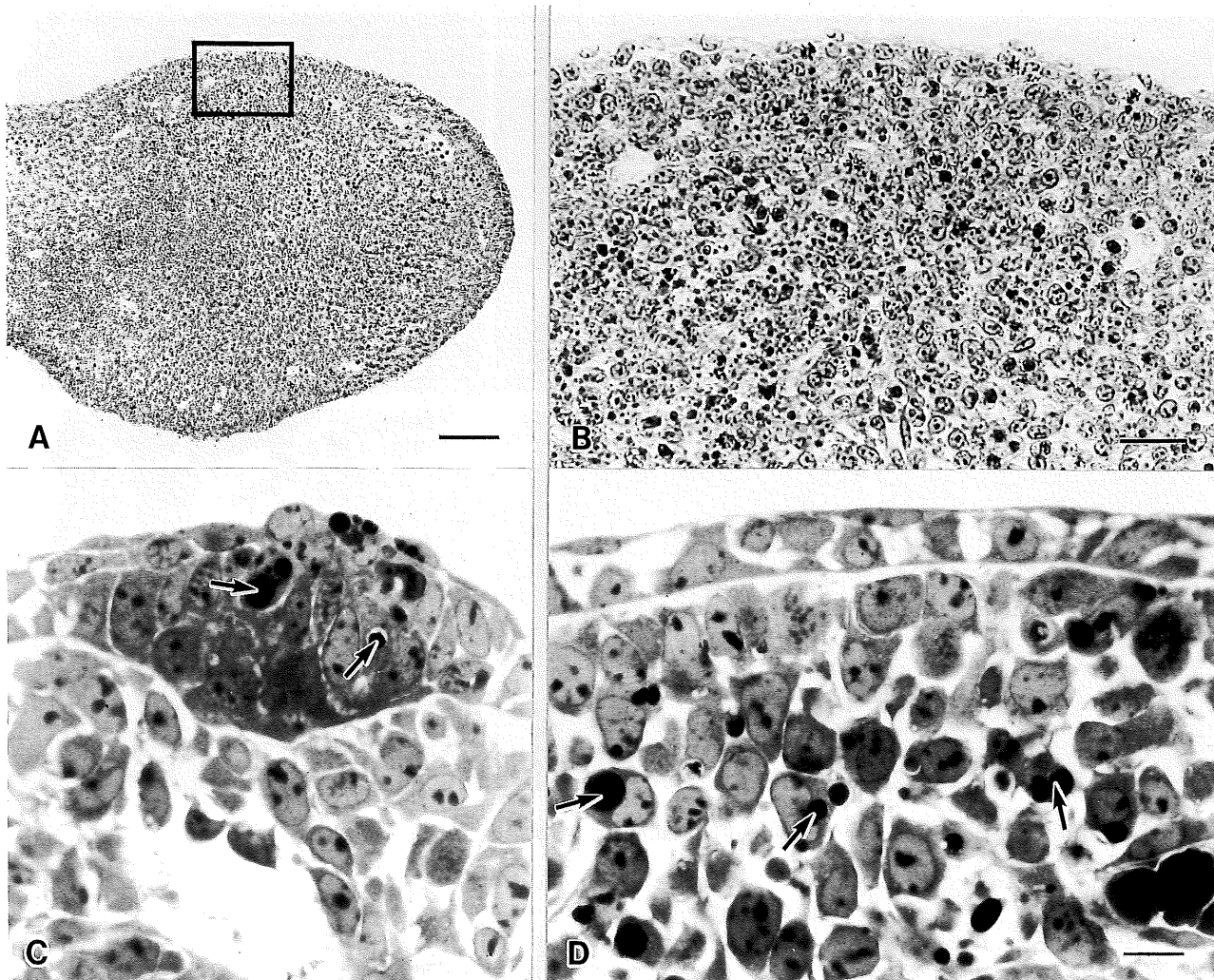


**Fig. 2.** Light micrographs of forelimb buds treated at gd 10.5, 6 hr after treatment.

A: A section parallel to the palmar plane. Note the distribution of dark staining bodies in the distal hand plate and preaxial area, representing dead and dying cells.

Scale bar = 100  $\mu$ m.

B: Higher magnification of the preaxial area boxed in A.

Scale bar = 25  $\mu$ m.

A, B: Stained with haematoxylin and eosin.

C: AER, note the number of pyknotic figures (arrows).

D: Mesenchymal area, note many pyknotic nuclei (arrows).

C, D: A section along the proximo-distal axis and perpendicular to the palmar plane, stained with toluidine blue.

Scale bar = 10  $\mu$ m for C and D.

### Light microscopic observations

The initial pathological change in limb buds after treatment with MAA was mesenchymal cell death. Pyknotic nuclei were observed throughout the limb mesenchyme 6 hr after treatment at gd 10.5, 11.0 or 11.5. The necrotic cells were frequently found in the distal and preaxial areas of limb buds (Fig. 2 A, B), and occasionally in the core. Cell death was also observed in the AER (Fig. 2 C).

### Scanning electron microscopic observations

External development of the control and MAA treated forelimbs is shown in Fig. 3. In the control embryos the AER on the forelimb became observable by gd 11.0 (Fig. 3 B). It was not so

conspicuous in comparison with that at gd 11.5. At gd 11.5 the forelimb bud showed a round shape hand plate (Fig. 3 C) with a well developed AER (Fig. 3 D). Involution of the AER occurred around gd 12.0 with formation of digital rays and interdigital notches at gd 12.5 (Fig. 3 E, F).

The forelimb buds from embryos treated with MAA at gd. 10.5 and observed 12 hr after treatment (Fig. 3 G, H) looked similar to those from controls. The limb buds 24 hr after treatment were smaller than those of controls, with hypoplasia of the AER (Fig. 3 I, J). The forelimbs 48 hr after treatment showed delayed formation of digital rays and interdigital notches (Fig. 3 K, L). In the peri-

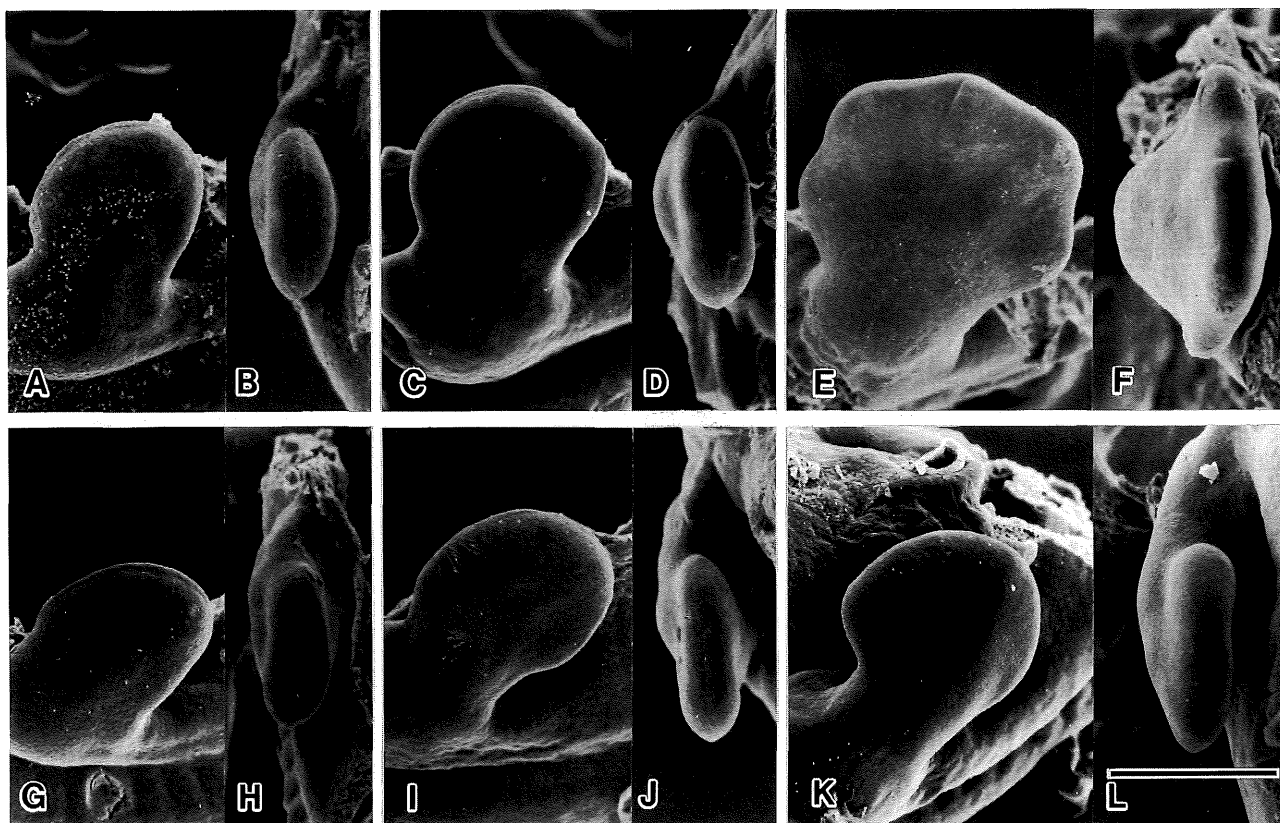


**Fig. 3.** Scanning electron micrographs of forelimb buds treated at gd 10.5.

A, C, E, G, I, K: Dorsal views.

B, D, F, H, J, L: Apical views.

A, B: 12 hr; C, D: 24 hr; E, F: 48 hr. Control series.

G, H: 12 hr; I, J: 24 hr; K, L: 48 hr. MAA treated series.

Note no apparent differences at 12 hr between control and treated ones.

I, J: 24 hr after treatment. Note small hand plate, and hypoplastic AER.

K, L: 48 hr after treatment. Note small hand plate, and late formation of digital rays.

Scale bar = 500  $\mu$ m.

derm covering the limb bud, no massive necrosis and cell debris were found, and the control and treated series showed no differences in appearance at higher magnifications (Fig. 4 C, D).

#### Transmission electron microscopic observations

The first sign of abnormality was observed in the mesenchyme (Fig. 5 D) and in the AER (Fig. 5 B) 2 hr after administration of MAA at gd 10.5. Some necrotic cells contained pyknotic nuclei and vacuoles. Some of the necrotic cells in the mesenchyme seemed to have been phagocytosed by neighboring mesenchymal cells.

#### DISCUSSION

The pathogenesis of limb malformations induced by metabolites of phthalate esters has been studied previously<sup>1,5</sup>. Scott et al<sup>5</sup> induced various limb malformations including ventral polydactyly of the hindlimb with 2-methoxyethanol (2-ME) in Wistar rats. They found that the limb bud periderm was severely damaged after the teratogen exposure, and they thought that the ventral duplication arose through an attempt by the embryo to repair the

periderm lesion. Greene et al<sup>1</sup> administered ethylene glycol monomethyl ether (synonym: 2-ME) to pregnant CD-1 mice, and examined histological changes in the embryonal mouse forelimb bud. They found that cell death was induced in the mesenchymal tissue and to some extent in the limb bud ectoderm, including the AER.

We gave a single oral dose of MAA to pregnant Jcl:ICR mice at gd 10.5, 11.0, or 11.5, and found that the degree of limb deformity was more severe when the teratogen was given at a later stage of gestation<sup>3</sup>. Our present observations clearly reveal that the initial pathological change is cell death in the limb mesenchyme and in the AER, and our findings are in accordance with those reported by Greene et al<sup>1</sup>. However, we did not detect any massive peridermal necrosis as mentioned by Scott et al<sup>5</sup>. This may be due to species differences between rat and mouse.

We gave MAA at three different developmental stages, and obtained different patterns of malformation, although the initial pathological changes seemed similar. We did not note any stage specif-

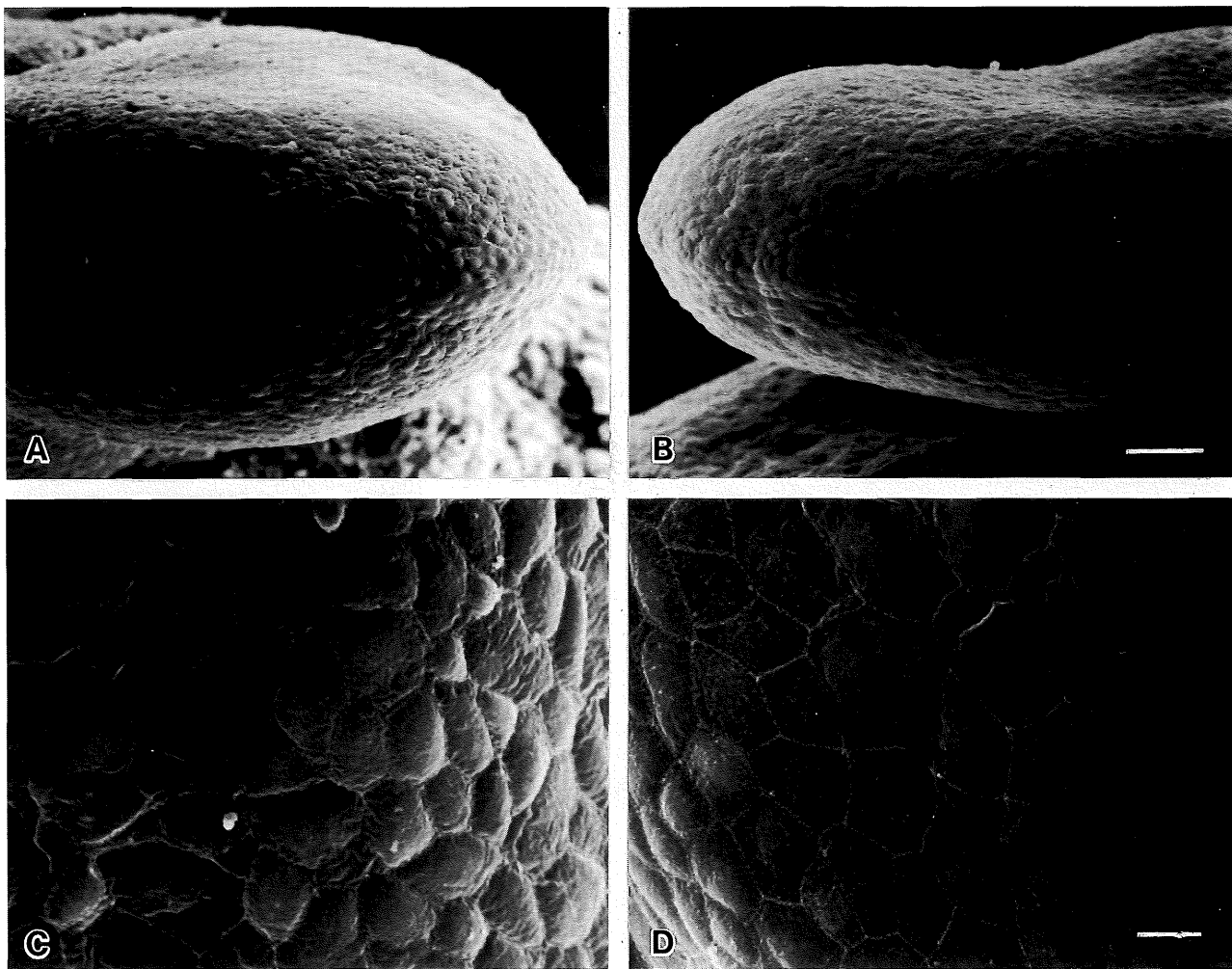


**Fig. 4.** Scanning electron micrographs of periderm covering the AER (A, B) and ventral areas (C, D) of the forelimb buds treated at gd 10.5, 12 hr after treatment.

A: Control; B: MAA treated. No apparent differences are noted between A and B.

C: Control; D: MAA treated. No apparent differences are noted between C and D. No massive cell necrosis was detected in B and D.

Scale bars = 50  $\mu\text{m}$  for A, B, and 10  $\mu\text{m}$  for C, D, respectively.

ic differences in the distribution of pathological cell death, whereas we noted some individual differences. How can we explain the fact that a similar initial change leads to different final defects? The recently established staging system for developing mouse limbs<sup>6</sup> and fate maps of mouse limbs<sup>2</sup> provide useful means of explaining this.

Forelimbs of Jcl:ICR mouse embryos at gd 10.5, 11.0, and 11.5 correspond to stages 4, 5, and 6 respectively according to Wanek et al<sup>6</sup>. Hindlimbs at gd 10.5, 11.0, and 11.5 correspond to stages 3, 4, and 5, respectively. According to the fate maps, presumptive carpal/tarsal and metacarpal/metatarsal elements have been laid down by stage 4/5, and presumptive phalangeal elements by stage 7/8. By their marking experiment, Muneoka et al<sup>2</sup> concluded that extensive cellular rearrangements did not occur during limb outgrowth. Thus we can predict the pattern of final defects from the initial distribution of cell death.

Of course we must consider the ability of the limb bud to regulate and regenerate after injury. Wanek et al<sup>7</sup> clearly demonstrated that the developing mouse limb at stage 7/8 was capable of partial regeneration of the peripheral digits following amputation. Genesis of intercalary defects induced by MAA can be explained by this regenerative capability.

Fig. 6 shows a scheme explaining the relation between initial cell death and final defects with reference to the treated stages and fate maps. When cells in the distal portion of a limb bud at stage 4 are damaged, the presumptive metacarpals suffer from the damage, and defects in the metacarpals result, while digital elements are formed by the regenerative capability of surviving cells in the distal area (Fig. 6, the forelimb treated at gd 10.5). If the damage is not extensive enough to produce complete loss of a digital ray, it may induce syndactyly. Preponderance of missing digits I and II

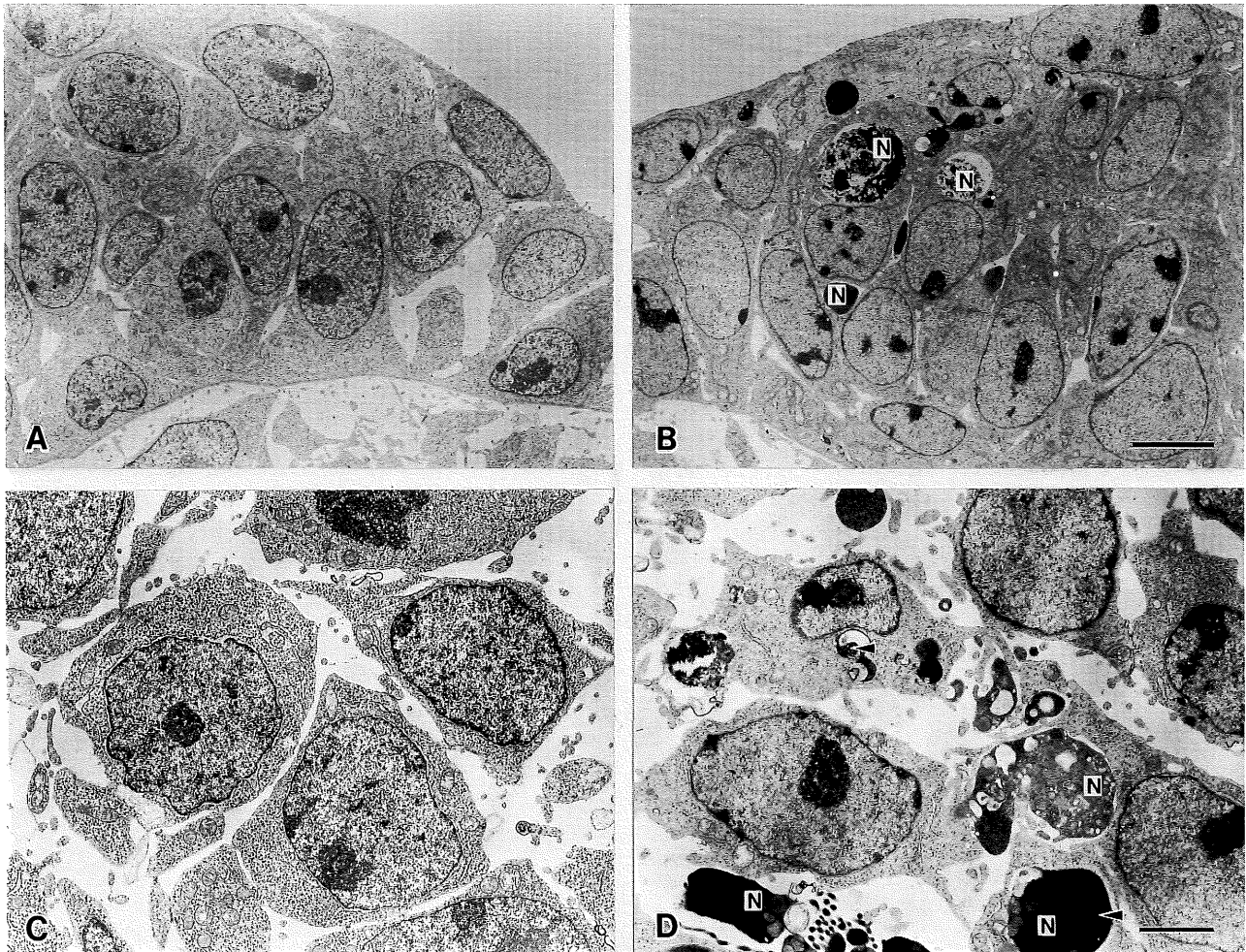


**Fig. 5.** Transmission electron micrographs of the AER (A, B) and mesenchymal areas (C, D) beneath the AER of the forelimb buds treated at gd 10.5, 2 hr after treatment.

A: Control; B: MAA treated. Necrotic cells (N) are observed.

C: Control. Round mesenchymal cells are observed with numerous free ribosomes. Some profiles of rough endoplasmic reticulum are also noticed.

D: MAA treated. Necrotic cells (N) are observed. They have higher electron density than healthy looking cells and contain some vacuoles. Some of the necrotic cells seem to be engulfed by neighboring mesenchymal cells (arrowheads).

Scale bars = 5  $\mu\text{m}$  for A, B, and 2.5  $\mu\text{m}$  for C, D, respectively.

reflects the preferential distribution of cell death to the preaxial area. Damages at later stages (Fig. 6, the forelimb treated at gd 11.0 or 11.5) result in more severe reduction deformities, because distal elements have been determined, the regenerative capacity has decreased by these stages, and the time for regeneration becomes shorter. Reduced sensitivity of the hindlimb to the teratogenicity of MAA may partly be explained by the delay in hindlimb development (Fig. 6, the hindlimb treated at gd 11.0). However, there seem to be factors involved other than the mere developmental delay of the hindlimb as compared with the forelimb. Limb defects induced in the hindlimb with treatment at gd 11.0 (stage 4) were less frequent and less severe than those induced in the forelimb with treatment at gd 10.5 (stage 4), although no differences were noted in the distribution of initial cell death

between the fore- and hindlimb. Quicker development of the hindlimb may be one of the factors which make the hindlimb more resistant to MAA teratogenesis.

The results obtained in this study indicate that cell necrosis in the developing limb results in various types of limb malformations according to the stage of injury, distribution, and regulation after the initial cell death. This information may be utilized for a better classification of human limb malformations.

#### ACKNOWLEDGMENTS

The authors wish to thank Mr. H. Maki and Mr. H. Ishihara, Department of Anatomy, Hiroshima University School of Medicine, for their technical assistance.

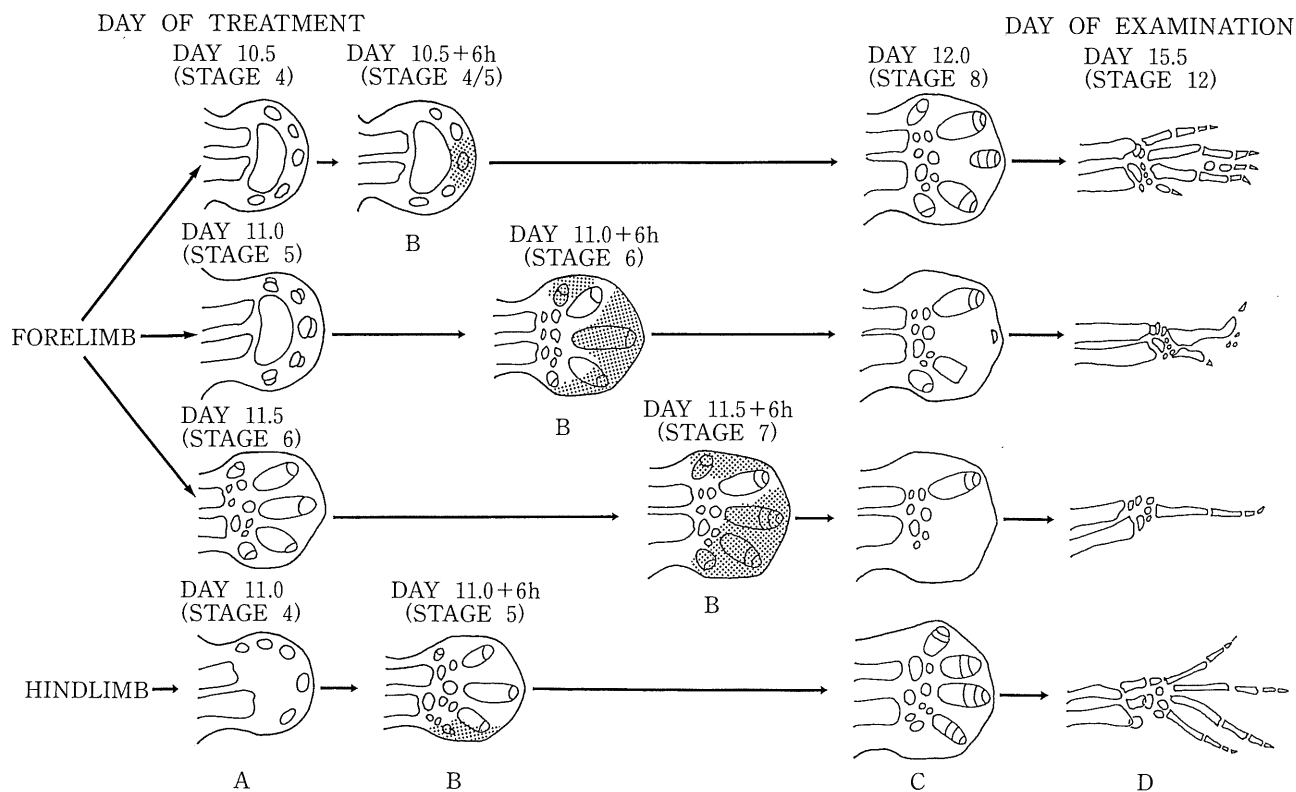


**Fig. 6.** Schematic drawings of relation between initial cell death and final defect of the limbs.

A: Fate maps at the time of treatment.

B: Initial cell death. Dots indicate distribution of cell death.

C: Defects in presumptive limb elements.

D: Final malformations.

This study was supported by Japan Society for the Promotion of Science (JSPS) RONPAKU (Dissertation Ph. D.) program and Hayashi's Foundation.

(Received May 15, 1991)

(Accepted June 13, 1991)

#### REFERENCES

1. Greene, J.A., Sleet, R.B., Morgan, K.T. and Welsch, F. 1987. Cytotoxic effects of ethylene glycol monomethyl ether in the forelimb bud of the mouse embryo. *Teratology* **36**: 23-34.
2. Muneoka, K., Wanek, N. and Bryant, S.V. 1989. Mammalian limb bud development: In situ fate maps of early hindlimb buds. *J. Exp. Zool.* **249**: 41-49.
3. Rasjad, C., Yamashita, K., Datu, A.R. and Yasuda, M. 1991. Patterns of limb malformations in mice induced by methoxyacetic acid. *Hiroshima J. Med. Sci.* **40**: 93-99.
4. Ritter, E.J., Scott, W.J. Jr., Randall, J.L. and Ritter, J.M. 1985. Teratogenicity of dimethoxyethyl phthalate and its metabolites methoxyethanol and methoxyacetic acid in the rat. *Teratology* **32**: 25-31.
5. Scott, W.J. Jr., Nau, H., Wittfoht, W. and Merker, H.J. 1987. Ventral duplication of the autopod: Chemical induction by methoxyacetic acid in rat embryos. *Development* **99**: 127-136.
6. Wanek, N., Muneoka, K., Holler-Dinsmore, G., Burton, R. and Bryant, S.V. 1989. A staging system for mouse limb development. *J. Exp. Zool.* **249**: 41-49.
7. Wanek, N., Muneoka, K. and Bryant, S.V. 1989. Evidence for regulation following amputation and tissue grafting in the developing mouse limb. *J. Exp. Zool.* **249**: 55-61.